Vol 15 No 1, January 2006
1009-1963/2006/15(01)/0022-13

Chinese Physics

© 2006 Chin. Phys. Soc.
and IOP Publishing Ltd

Numerical method of the Riemann problem for two-dimensional multi-fluid flows with general equation of state*

Bai Jing-Song(柏劲松)†, Zhang Zhan-Ji(张展冀),
Li Ping(李 平), and Zhong Min(钟 敏)

Laboratory for Shock Wave and Detonation Physics Research, Institute of Fluid Physics, Mianyang 621900, China

(Received 2 February 2005; revised manuscript received 8 October 2005)

Based on the classical Roe method, we develop an interface capture method according to the general equation of state, and extend the single-fluid Roe method to the two-dimensional (2D) multi-fluid flows, as well as construct the continuous Roe matrix for the whole flow field. The interface capture equations and fluid dynamic conservative equations are coupled together and solved by using any high-resolution schemes that usually suit for the single-fluid flows. Some numerical examples are given to illustrate the solution of 1D and 2D multi-fluid Riemann problems.

Keywords: Riemann problem, multi-fluid flows, Roe scheme, general equation of state
PACC: 0340G, 5235T

1. Introduction

Many problems in science and engineering involve conservation laws. A special class is the so-called hyperbolic conservation laws, which can be formulated as a system of partial differential equations. In general it is not possible to derive exact solutions of these equations, and therefore, we have to devise and study numerical methods to obtain approximate solutions. The interaction of elementary waves for systems in the hyperbolic conservation laws is the key mechanism in determining the qualitative properties of solutions. Riemann studied fluid dynamics through the shock tube experiment. More generally, a Riemann problem for a system in conservation laws is an initial value problem such as wave structure of hyperbolic partial differential equations. They are important also for numerical algorithms for solving these equations, such as the Godunov method, the random choice method and the front tracking method. These solutions, in turn, are composed of elementary waves, whose interactions are determined by Riemann problems, also reflect the asymptotic behaviour of general solutions. Therefore the influence of an equation of state on the structure of waves may be studied through Riemann problems.

It is known that it is difficult to obtain the exact solution of the Riemann problem, especially for the multi-fluid flow with general equation of state (EOS). A perfectly general EOS is also capable of exhibiting pathological behaviour that leads to complicated and non-unique solutions of the Riemann problem.[1,2] Only the simple EOS can be solved accurately through iterative procedure.[3] Usually, some approximate methods are introduced to the Riemann problem, such as Roe method and two-shock method,[4−6] etc. Based on the approximate Riemann solvers, many high-resolution Euler schemes (for example, TVD, MUSCL and PPM schemes, etc) appeared and a lot of excellent numerical results to the single-fluid flows are obtained. For different materials corresponding to the different EOS in multi-fluid flows, the numerical flux becomes discontinuous at the boundary of different fluids, so there exists no flux matrix in the multi-fluid problem. The volume-of-fraction (VOF) method is a popular and successful technique to describe the multi-fluid flows.[7−10] The algorithm captures rather than tracks the interfaces between distinct fluids while maintaining a VOF representation of the constituent fluids. The simplest

*Project supported by the Foundation of China Academy of Engineering Physics (Grant No 20040650 and 2003-421050501-1-05).
†E-mail: bjsong_mail@21cn.com

VOF interface reconstruction algorithms are those based on the simple line interface calculation (SLIC) method.[11] There are numerous other first-order variations on this, such as the centre of mass method,[12] centre difference[13] and Young's method.[14] The primary disadvantage in using these methods is the expense. Reconstruction of the interface adds more computation than simply advances the flow in time. In addition, the reconstruction process is performed on a cell by cell basis and hence requires some coding sophistication so that vectorization can be achieved on modern supercomputers. Recently, with the remarkable permeation of artificial intelligence among various fields of science and engineering, including fluid mechanics, symbolic computation has drastically increased the ability of a computer to exactly and algorithmically deal with the analytic expressions, as shown in Refs.[15–17].

In this paper, we develop the interface capture method according to the general EOS, and extend the single-fluid Roe method to the two-dimensional (2D) multi-fluid flows, as well as construct the continuous Roe matrix to the whole flow field. The interface capture equations and fluid dynamic conservative equations are coupled together and solved by using any high-resolution schemes that usually suit for the single-fluid flows. We apply the basic symbolic computation method to our algorithms and deduce a set of formulas that is directly used in the numerical schemes. The processes of construction of the Roe matrix, eigenvalue and eigenvector for the multi-fluid flow by stiffen gas, polynomial and Grüneisen (including Jones–Wilkins–Lee abbreviated as JWL) EOS in two dimensions are presented. Finally some numerical examples for solving the Riemann problem in 1D and 2D multi-fluid flows with the above EOSs are given, too.

2. Interface capture equation with general EOS

The form of the general EOS in this paper is

$$p = \Omega(\rho, e, a_1, \cdots, a_n) + \Theta(\rho, e, b_1, \cdots, b_n)e, \quad (1)$$

where p, ρ, e represent the pressure, density and specific internal energy, respectively; a_i and b_i are independent parameters, associated with each material. The typical EOS includes stiffen gas, polynomial and Grüneisen EOS, etc. For the stiffened gas case,

$$\rho e = (p + \gamma\pi)/(\gamma - 1), \quad (2)$$

where π is the material-dependent parameter, γ represents the ratio of specific heats for the gas. And for the polynomial EOS,

$$\begin{aligned} p =& a_0 + a_1\rho + a_2\rho^2 + a_3\rho^3 \\ &+ (b_0 + b_1\rho + b_2\rho^2 + b_3\rho^3)e, \end{aligned} \quad (3)$$

where a_i, $b_i (i = 0, \cdots, 3)$ are material-dependent parameters. For the Grüneisen EOS

$$p(\rho, e) = p_{\rm ref}(\rho) + \Gamma(\rho)\rho[e - e_{\rm ref}(\rho)], \quad (4)$$

where $\Gamma(\rho) = (\partial p/\partial e)_\rho/\rho$ is the Grüneisen coefficient, $p_{\rm ref}$, $e_{\rm ref}$ are the reference state of pressure and specific internal energy along the Hugoniot respectively.

For a solid material such as metal, a linear fit assumption is made for shock velocity as a function of the particle velocity, i.e.

$$u_s = c_0 + \lambda u_{\rm p}. \quad (5)$$

Here $u_{\rm s}$ represents the shock velocity, c_0 is the zero-pressure isentropic speed of sound, and λ is a dimensionless parameter related to the pressure derivative of the isentropic bulk modulus. By virtue of Eq.(5), it is easy to deduce that the reference curve for ($p_{\rm ref}$, $e_{\rm ref}$) is simply a single Hugoniot locus from an initial point (p_0, e_0). With this in mind, using the standard Rankine–Hugoniot jump condition, and after some simple algebraic manipulations, we can find the explicit expression for $p_{\rm ref}$ and $e_{\rm ref}$ as

$$\begin{aligned} \Gamma(V) =& \Gamma_0 \left(\frac{V}{V_0}\right)^\alpha, \\ p_{\rm ref}(V) =& p_0 + \frac{c_0^2(V_0 - V)}{[V_0 - \lambda(V_0 - V)]}, \\ e_{\rm ref}(V) =& e_0 + \frac{1}{2}\left[p_{\rm ref}(V) + p_0\right](V_0 - V), \end{aligned} \quad (6)$$

where $V = 1/\rho$ represents the volume, $\Gamma_0 = \gamma_0 - 1$ represents the Grüneisen coefficient at volume $V = V_0$, $\gamma_0 > 1$ is the usual definition of the ratio of specific heats, and $\alpha \in [0, 1]$ is a dimensionless parameter.

For the gaseous explosive with Jones–Wilkins–Lee (JWL) equation of state, $p_{\rm ref}, e_{\rm ref}$ and $\Gamma(V)$ in Eq.(4) are

$$\begin{aligned} \Gamma(V) =& \Gamma_0, \\ e_{\rm ref}(V) =& \frac{AV_0}{R_1}\exp\left(\frac{-R_1V}{V_0}\right) \\ &+ \frac{BV_0}{R_2}\exp\left(\frac{-R_2V}{V_0}\right) - e_0, \\ p_{\rm ref}(V) =& A\exp\left(\frac{-R_1V}{V_0}\right) + B\exp\left(\frac{-R_2V}{V_0}\right), \end{aligned} \quad (7)$$

where Γ_0, V_0, e_0, A, B, R_1, R_2 are seven material-dependent parameters.

Without viscosity and heat conduction, the conservation Euler equations for a compressible fluid are

$$\begin{cases} \dfrac{\partial \rho}{\partial t} + \nabla \cdot (\rho \boldsymbol{v}) = 0, \\ \dfrac{\partial \rho \boldsymbol{v}}{\partial t} + \nabla \cdot (\rho \boldsymbol{v} v) = -\nabla p, \\ \dfrac{\partial \rho E}{\partial t} + \nabla \cdot (\rho E \boldsymbol{v}) = -\nabla (p \boldsymbol{v}), \end{cases} \tag{8}$$

where $\boldsymbol{v}$ is velocity vector, E is the total energy for unit mass, $E = \rho e + \rho \boldsymbol{v}^2/2$.

At the multi-fluid interface, weak discontinuities exist physically. For numerical dissipation of difference scheme, there are $|\nabla p| \sim 1$, $|\nabla |\boldsymbol{v}|| \sim 1$, $|\nabla e| \gg 1, |\nabla \rho| \gg 1$ near the interface field. Therefore, we may assume that p and $\boldsymbol{v}$ are constant near the interface field, then Eq.(8) can be written as

$$\begin{cases} \dfrac{\partial \rho}{\partial t} + \boldsymbol{v} \cdot \nabla \rho = 0, \\ \dfrac{\partial}{\partial t}(\rho e) + \boldsymbol{v} \cdot \nabla (\rho e) = 0. \end{cases} \tag{9}$$

Using Eq.(1) and the second formula of Eq.(9), we have

$$\frac{\partial}{\partial t}\left(\rho \frac{p - \Omega}{\Theta}\right) + \boldsymbol{v} \cdot \nabla \left(\rho \frac{p - \Omega}{\Theta}\right) = 0. \tag{10}$$

Since p and $\boldsymbol{v}$ are constant, Eq.(10) can be rewritten as

$$\begin{cases} \dfrac{\partial}{\partial t}\left(\dfrac{\rho}{\Theta}\right) + \nabla \cdot \left(\dfrac{\rho}{\Theta}\boldsymbol{v}\right) = 0, \\ \dfrac{\partial}{\partial t}\left(\dfrac{\rho \Omega}{\Theta}\right) + \nabla \cdot \left(\dfrac{\rho \Omega}{\Theta}\boldsymbol{v}\right) = 0. \end{cases} \tag{11}$$

Generally, when p and $\boldsymbol{v}$ are not constant, the left-hand side of Eq.(11) becomes

$$\begin{cases} \dfrac{\partial}{\partial t}\left(\dfrac{\rho}{\Theta}\right) + \nabla \cdot \left(\dfrac{\rho}{\Theta}\boldsymbol{v}\right) = \rho \dfrac{\partial}{\partial t}\left(\dfrac{1}{\Theta}\right) + \rho \mathbf{v} \cdot \nabla \left(\dfrac{1}{\Theta}\right) = \rho \dfrac{d}{dt}\left(\dfrac{1}{\Theta}\right), \\ \dfrac{\partial}{\partial t}\left(\dfrac{\rho \Omega}{\Theta}\right) + \nabla \cdot \left(\dfrac{\rho \Omega}{\Theta}\boldsymbol{v}\right) = \rho \dfrac{\partial}{\partial t}\left(\dfrac{\Omega}{\Theta}\right) + \rho \boldsymbol{v} \cdot \nabla \left(\dfrac{\Omega}{\Theta}\right) = \rho \dfrac{d}{dt}\left(\dfrac{\Omega}{\Theta}\right). \end{cases} \tag{12}$$

By combining the mass conservation equation with the energy equation of $\mathrm{d}e/\mathrm{d}t = -p\mathrm{d}(1/\rho)\mathrm{d}t$, the first formula of Eq.(12) can be written as

$$\begin{aligned} \rho \frac{\partial}{\partial t}\left(\frac{1}{\Theta}\right) + \rho \boldsymbol{v} \cdot \nabla \left(\frac{1}{\Theta}\right) =& \rho \frac{\mathrm{d}}{\mathrm{d}t}\left(\frac{1}{\Theta}\right) = \rho \frac{\partial}{\partial \rho}\left(\frac{1}{\Theta}\right)\frac{\mathrm{d}\rho}{\mathrm{d}t} + \rho \frac{\partial}{\partial e}\left(\frac{1}{\Theta}\right)\frac{\mathrm{d}e}{\mathrm{d}t} \\ =& \left(\rho \frac{\partial}{\partial \rho}\left(\frac{1}{\Theta}\right) + \frac{p}{\rho}\frac{\partial}{\partial e}\left(\frac{1}{\Theta}\right)\right)\frac{\mathrm{d}\rho}{\mathrm{d}t} = -\left[\rho^2 \frac{\partial}{\partial \rho}\left(\frac{1}{\Theta}\right) + p \frac{\partial}{\partial e}\left(\frac{1}{\Theta}\right)\right]\nabla \cdot \boldsymbol{v}. \end{aligned} \tag{13}$$

Analogously, the second formula of Eq.(12) can be written as follows:

$$\begin{cases} \rho \dfrac{\partial}{\partial t}\left(\dfrac{1}{\Theta}\right) + \rho \boldsymbol{v} \cdot \nabla \left(\dfrac{1}{\Theta}\right) = \rho \dfrac{\mathrm{d}}{\mathrm{d}t}\left(\dfrac{1}{\Theta}\right) = -\left[\rho^2 \dfrac{\partial}{\partial \rho}\left(\dfrac{1}{\Theta}\right) + p \dfrac{\partial}{\partial e}\left(\dfrac{1}{\Theta}\right)\right]\nabla \cdot \boldsymbol{v}, \\ \rho \dfrac{\partial}{\partial t}\left(\dfrac{\Omega}{\Theta}\right) + \rho \boldsymbol{v} \cdot \nabla \left(\dfrac{\Omega}{\Theta}\right) = \rho \dfrac{\mathrm{d}}{\mathrm{d}t}\left(\dfrac{\Omega}{\Theta}\right) = -\left[\rho^2 \dfrac{\partial}{\partial \rho}\left(\dfrac{\Omega}{\Theta}\right) + p \dfrac{\partial}{\partial e}\left(\dfrac{\Omega}{\Theta}\right)\right]\nabla \cdot \boldsymbol{v}. \end{cases} \tag{14}$$

Finally, we obtain the interface equivalent equation from Eqs.(12)–(14),

$$\begin{cases} \dfrac{\partial}{\partial t}\left(\dfrac{\rho}{\Theta}\right) + \nabla \cdot \left(\dfrac{\rho}{\Theta}\boldsymbol{v}\right) + \left[\rho^2 \dfrac{\partial}{\partial \rho}\left(\dfrac{1}{\Theta}\right) + p \dfrac{\partial}{\partial e}\left(\dfrac{1}{\Theta}\right)\right]\nabla \cdot \boldsymbol{v} = 0, \\ \dfrac{\partial}{\partial t}\left(\dfrac{\rho \Omega}{\Theta}\right) + \nabla \cdot \left(\dfrac{\rho \Omega}{\Theta}\boldsymbol{v}\right) + \left[\rho^2 \dfrac{\partial}{\partial \rho}\left(\dfrac{\Omega}{\Theta}\right) + p \dfrac{\partial}{\partial e}\left(\dfrac{\Omega}{\Theta}\right)\right]\nabla \cdot \boldsymbol{v} = 0; \end{cases} \tag{15}$$

or

$$\begin{cases} \dfrac{\partial}{\partial t}\left(\dfrac{1}{\Theta}\right) + \boldsymbol{v} \cdot \nabla \left(\dfrac{1}{\Theta}\right) + \left[\rho \dfrac{\partial}{\partial \rho}\left(\dfrac{1}{\Theta}\right) + \dfrac{p}{\rho}\dfrac{\partial}{\partial e}\left(\dfrac{1}{\Theta}\right)\right]\nabla \cdot \boldsymbol{v} = 0, \\ \dfrac{\partial}{\partial t}\left(\dfrac{\Omega}{\Theta}\right) + \boldsymbol{v} \cdot \nabla \left(\dfrac{\Omega}{\Theta}\right) + \left[\rho \dfrac{\partial}{\partial \rho}\left(\dfrac{\Omega}{\Theta}\right) + \dfrac{p}{\rho}\dfrac{\partial}{\partial e}\left(\dfrac{\Omega}{\Theta}\right)\right]\nabla \cdot \boldsymbol{v} = 0. \end{cases} \tag{16}$$

3. Roe matrix construction of Riemann problem for multi-fluid flows

Coupling Eq.(8) with Eq.(9), we have the quasi-linear equation,

$$\frac{\partial \tilde{\boldsymbol{q}}}{\partial t}+\sum_{\nu=1}^{N}\tilde{\boldsymbol{A}}_{\nu}\left(\tilde{\boldsymbol{q}}\right)\frac{\partial \tilde{\boldsymbol{q}}}{\partial x_{\nu}}=\boldsymbol{0}, \tag{17}$$

where $\tilde{\boldsymbol{A}}_{\nu}$ is the Roe matrix, $\tilde{\boldsymbol{q}}$ and $\tilde{\boldsymbol{A}}_{\nu}\left(\tilde{\boldsymbol{q}}\right)$ depend on the specific EOS. Next, the processes and results of construction of the Roe matrix, eigenvalue and eigenvector for the multi-fluid flow by stiffened gas, polynomial and Grüneisen EOS in two dimensions are given separately. For stiffened gas EOS, we have

$$\tilde{\boldsymbol{q}}=\left[\tilde{\rho},\tilde{\rho}\tilde{u},\tilde{\rho}\tilde{v},\tilde{\rho}\tilde{E},1/(\tilde{\gamma}-1),\tilde{\gamma}\tilde{\pi}/\tilde{\gamma}-1\right]^{\mathrm{T}},$$

$$\tilde{\boldsymbol{A}}=\begin{bmatrix}0 & 1 & 0 & 0 & 0 & 0\\ \tilde{\beta}^2-\tilde{u}^2 & (3-\tilde{\gamma})\,\tilde{u} & (1-\tilde{\gamma})\,\tilde{v} & \tilde{\gamma}-1 & \tilde{\chi} & 1-\tilde{\gamma}\\ -\tilde{u}\tilde{v} & \tilde{v} & \tilde{u} & 0 & 0 & 0\\ \left(\tilde{\beta}^2-\tilde{H}\right)\tilde{u} & \tilde{H}-(\tilde{\gamma}-1)\,\tilde{u}^2 & (1-\tilde{\gamma})\,\tilde{u}\tilde{v} & \tilde{\gamma}\tilde{u} & \tilde{\chi}\tilde{u} & (1-\tilde{\gamma})\,\tilde{u}\\ 0 & 0 & 0 & 0 & \tilde{u} & 0\\ 0 & 0 & 0 & 0 & 0 & \tilde{u}\end{bmatrix}, \tag{18}$$

$$\tilde{\boldsymbol{B}}=\begin{bmatrix}0 & 0 & 1 & 0 & 0 & 0\\ -\tilde{u}\tilde{v} & \tilde{v} & \tilde{u} & 0 & 0 & 0\\ \tilde{\beta}^2-\tilde{v}^2 & (1-\tilde{\gamma})\,\tilde{u} & (3-\tilde{\gamma})\,\tilde{v} & \tilde{\gamma}-1 & \tilde{\chi} & 1-\tilde{\gamma}\\ \left(\tilde{\beta}^2-\tilde{H}\right)\tilde{v} & (1-\tilde{\gamma})\,\tilde{u}\tilde{v} & H-(\tilde{\gamma}-1)\,v^2 & (\tilde{\gamma}-1)\,\tilde{v} & \tilde{\chi}\tilde{v} & (1-\tilde{\gamma})\,\tilde{v}\\ 0 & 0 & 0 & 0 & \tilde{v} & 0\\ 0 & 0 & 0 & 0 & 0 & \tilde{v}\end{bmatrix}. \tag{19}$$

Here $\tilde{\boldsymbol{A}}$ and $\tilde{\boldsymbol{B}}$ represent the x-direction and y-direction Roe matrix (as below). $\tilde{\chi}=-\tilde{I}/(\tilde{\gamma}-1)^2$, $\tilde{I}=\tilde{p}/(\tilde{\gamma}-1)$, $\tilde{\beta}^2=(\tilde{\gamma}-1)\left(\tilde{u}^2+\tilde{v}^2\right)/2$, $\tilde{c}=(\tilde{\gamma}-1)\sqrt{\tilde{H}-(\tilde{u}^2+\tilde{v}^2)/2}$, $\tilde{H}=\tilde{E}+\tilde{p}/\tilde{\rho}$. The variable with "$\sim$" represents the result by the classical Roe method. The right eigenvectors of matrix $\tilde{\boldsymbol{A}}$ and $\tilde{\boldsymbol{B}}$ are $\tilde{\boldsymbol{R}}_A$ for $\tilde{\boldsymbol{r}}_A^p(p=1-6)$ and $\tilde{\boldsymbol{R}}_B$ for $\tilde{\boldsymbol{r}}_B^p(p=1-6)$,

$$\tilde{\boldsymbol{R}}_A=\left[\tilde{\boldsymbol{r}}_A^1\middle|\,\tilde{\boldsymbol{r}}_A^2\middle|\,\tilde{\boldsymbol{r}}_A^3\middle|\,\tilde{\boldsymbol{r}}_A^4\middle|\,\tilde{\boldsymbol{r}}_A^5\middle|\,\tilde{\boldsymbol{r}}_A^6\right]=\begin{bmatrix}1 & 0 & 1 & 1 & 0 & 0\\ \tilde{u}-\tilde{c} & 0 & \hat{u} & \tilde{u}+\tilde{c} & 0 & 0\\ \tilde{v} & 1 & \tilde{v} & \tilde{v} & 0 & 0\\ \tilde{H}-\tilde{u}\tilde{c} & \tilde{v} & \frac{1}{2}\left(\tilde{u}^2+\tilde{v}^2\right) & \tilde{H}+\tilde{u}\tilde{c} & \tilde{p} & 1\\ 0 & 0 & 0 & 0 & 1 & 0\\ 0 & 0 & 0 & 0 & 0 & 1\end{bmatrix},$$

$$\tilde{\boldsymbol{R}}_B=\left[\tilde{\boldsymbol{r}}_B^1\middle|\,\tilde{\boldsymbol{r}}_B^2\middle|\,\tilde{\boldsymbol{r}}_B^3\middle|\,\tilde{\boldsymbol{r}}_B^4\middle|\,\tilde{\boldsymbol{r}}_B^5\middle|\,\tilde{\boldsymbol{r}}_B^6\right]=\begin{bmatrix}1 & 0 & 1 & 1 & 0 & 0\\ \tilde{u} & 1 & \tilde{u} & \hat{u} & 0 & 0\\ \tilde{v}-\tilde{c} & 0 & \tilde{v} & \tilde{v}+\tilde{c} & 0 & 0\\ \tilde{H}-\tilde{v}\tilde{c} & \tilde{u} & \frac{1}{2}\left(\tilde{u}^2+\tilde{v}^2\right) & \tilde{H}+\tilde{v}\tilde{c} & \tilde{p} & 1\\ 0 & 0 & 0 & 0 & 1 & 0\\ 0 & 0 & 0 & 0 & 0 & 1\end{bmatrix}. \tag{20}$$

For the polynomial EOS, $\tilde{\boldsymbol{q}}$, $\tilde{\boldsymbol{A}}$ and $\tilde{\boldsymbol{B}}$ are as follows:

$$\tilde{\boldsymbol{q}} = \left[\tilde{\rho}, \tilde{\rho}\tilde{u}, \tilde{\rho}\tilde{v}, \tilde{\rho}\tilde{E}, \frac{\tilde{\rho}}{\tilde{\Theta}(\tilde{\rho})}, \frac{a_0\tilde{\rho}}{\tilde{\Theta}(\tilde{\rho})}, \frac{a_1\tilde{\rho}^2}{\tilde{\Theta}(\tilde{\rho})}, \frac{a_2\tilde{\rho}^3}{\tilde{\Theta}(\tilde{\rho})}, \frac{a_3\tilde{\rho}^4}{\tilde{\Theta}(\tilde{\rho})}, \tilde{b}_0, \tilde{b}_1, \tilde{b}_2, \tilde{b}_3\right]^{\mathrm{T}}, \tag{21}$$

$$\tilde{\boldsymbol{A}} = \begin{bmatrix}
0 & 1 & 0 & 0 & 0 & 0 & 0 & 0 & 0 & 0 & 0 & 0 & 0 \\
\tilde{\delta}_1\tilde{\delta}_2 - \tilde{u}^2 & (2-\tilde{\delta}_1)\tilde{u} & -\tilde{\delta}_1\tilde{v} & \tilde{\delta}_1 & -\tilde{\delta}_1\tilde{p} & \tilde{\delta}_1 & \tilde{\delta}_1 & \tilde{\delta}_1 & \tilde{\delta}_1 & 0 & 0 & 0 & 0 \\
-\tilde{u}\tilde{v} & \tilde{v} & u & 0 & 0 & 0 & 0 & 0 & 0 & 0 & 0 & 0 & 0 \\
\left(\tilde{\delta}_1\tilde{\delta}_2 - \tilde{H}\right)u & \tilde{H} - \tilde{\delta}_1\tilde{u}^2 & -\tilde{\delta}_1\tilde{u}\tilde{v} & (1+\tilde{\delta}_1)\tilde{u} & -\tilde{\delta}_1\tilde{p}\tilde{u} & \tilde{\delta}_1\tilde{u} & \tilde{\delta}_1\tilde{u} & \tilde{\delta}_1\tilde{u} & \tilde{\delta}_1\tilde{u} & 0 & 0 & 0 & 0 \\
-\tilde{\varphi}_1\tilde{u} & \tilde{\varphi}_1 & 0 & 0 & \tilde{u} & 0 & 0 & 0 & 0 & 0 & 0 & 0 & 0 \\
-\tilde{\varphi}_2\tilde{u} & \tilde{\varphi}_2 & 0 & 0 & 0 & \tilde{u} & 0 & 0 & 0 & 0 & 0 & 0 & 0 \\
-\tilde{\varphi}_3\tilde{u} & \tilde{\varphi}_3 & 0 & 0 & 0 & 0 & \tilde{u} & 0 & 0 & 0 & 0 & 0 & 0 \\
-\tilde{\varphi}_4\tilde{u} & \tilde{\varphi}_4 & 0 & 0 & 0 & 0 & 0 & \tilde{u} & 0 & 0 & 0 & 0 & 0 \\
-\tilde{\varphi}_5\tilde{u} & \tilde{\varphi}_5 & 0 & 0 & 0 & 0 & 0 & 0 & \tilde{u} & 0 & 0 & 0 & 0 \\
0 & 0 & 0 & 0 & 0 & 0 & 0 & 0 & 0 & \tilde{u} & 0 & 0 & 0 \\
0 & 0 & 0 & 0 & 0 & 0 & 0 & 0 & 0 & 0 & \tilde{u} & 0 & 0 \\
0 & 0 & 0 & 0 & 0 & 0 & 0 & 0 & 0 & 0 & 0 & \tilde{u} & 0 \\
0 & 0 & 0 & 0 & 0 & 0 & 0 & 0 & 0 & 0 & 0 & 0 & \tilde{u}
\end{bmatrix}, \tag{22}$$

$$\tilde{\boldsymbol{B}} = \begin{bmatrix}
0 & 0 & 1 & 0 & 0 & 0 & 0 & 0 & 0 & 0 & 0 & 0 & 0 \\
-\tilde{u}\tilde{v} & \tilde{v} & \tilde{u} & 0 & 0 & 0 & 0 & 0 & 0 & 0 & 0 & 0 & 0 \\
\tilde{\delta}_1\tilde{\delta}_2 - \tilde{v}^2 & -\tilde{\delta}_1\tilde{u} & (2-\tilde{\delta}_1)\tilde{v} & \tilde{\delta}_1 & -\tilde{\delta}_1\tilde{p} & \tilde{\delta}_1 & \tilde{\delta}_1 & \tilde{\delta}_1 & \tilde{\delta}_1 & 0 & 0 & 0 & 0 \\
\left(\tilde{\delta}_1\tilde{\delta}_2 - \tilde{H}\right)\tilde{v} & -\tilde{\delta}_1\tilde{u}\tilde{v} & \tilde{H} - \tilde{\delta}_1\tilde{v}^2 & (1+\tilde{\delta}_1)\tilde{v} & -\tilde{\delta}_1 p\tilde{v} & \tilde{\delta}_1\tilde{v} & \tilde{\delta}_1\tilde{v} & \tilde{\delta}_1\tilde{v} & \tilde{\delta}_1\tilde{v} & 0 & 0 & 0 & 0 \\
-\tilde{\varphi}_1\tilde{v} & 0 & \tilde{\varphi}_1 & 0 & \tilde{v} & 0 & 0 & 0 & 0 & 0 & 0 & 0 & 0 \\
-\tilde{\varphi}_2\tilde{v} & 0 & \tilde{\varphi}_2 & 0 & 0 & \tilde{v} & 0 & 0 & 0 & 0 & 0 & 0 & 0 \\
-\tilde{\varphi}_3\tilde{v} & 0 & \tilde{\varphi}_3 & 0 & 0 & 0 & \tilde{v} & 0 & 0 & 0 & 0 & 0 & 0 \\
-\tilde{\varphi}_4\tilde{v} & 0 & \tilde{\varphi}_4 & 0 & 0 & 0 & 0 & \tilde{v} & 0 & 0 & 0 & 0 & 0 \\
-\tilde{\varphi}_5\tilde{v} & 0 & \tilde{\varphi}_5 & 0 & 0 & 0 & 0 & 0 & \tilde{v} & 0 & 0 & 0 & 0 \\
0 & 0 & 0 & 0 & 0 & 0 & 0 & 0 & 0 & \tilde{v} & 0 & 0 & 0 \\
0 & 0 & 0 & 0 & 0 & 0 & 0 & 0 & 0 & 0 & \tilde{v} & 0 & 0 \\
0 & 0 & 0 & 0 & 0 & 0 & 0 & 0 & 0 & 0 & 0 & \tilde{v} & 0 \\
0 & 0 & 0 & 0 & 0 & 0 & 0 & 0 & 0 & 0 & 0 & 0 & \tilde{v}
\end{bmatrix}, \tag{23}$$

where $\tilde{\delta}_1 = \tilde{\Theta}(\tilde{\rho})/\tilde{\rho}$, $\tilde{\delta}_2 = (\tilde{u}^2+\tilde{v}^2)/2$, $\tilde{\varphi}_1 = (\tilde{\Theta}(\tilde{\rho}) - \tilde{\rho}\tilde{\Theta}'(\tilde{\rho}))/\tilde{\Theta}(\tilde{\rho})^2$, $\tilde{\varphi}_2 = \tilde{\varphi}_1\tilde{a}_0$, $\tilde{\varphi}_3 = \tilde{a}_1\tilde{\rho}/\tilde{\Theta}(\tilde{\rho}) + \tilde{\varphi}_1\tilde{a}_1\tilde{\rho}$, $\tilde{\varphi}_4 = 2\tilde{a}_2\tilde{\rho}^2/\tilde{\Theta}(\tilde{\rho}) + \tilde{\varphi}_1\tilde{a}_2\tilde{\rho}^2$, $\tilde{\varphi}_5 = 3\tilde{a}_3\tilde{\rho}^3/\tilde{\Theta}(\tilde{\rho}) + \tilde{\varphi}_1\tilde{a}_3\tilde{\rho}^3$, $\tilde{c} = \sqrt{\tilde{\delta}_1\left(\tilde{H} - \tilde{p}\tilde{\varphi}_1 + \tilde{\varphi}_2 + \tilde{\varphi}_3 + \tilde{\varphi}_4 + \tilde{\varphi}_5 - (\tilde{u}^2+\tilde{v}^2)/2\right)}$. The right eigenvector corresponding to eigenvalue of Roe matrix is,

$$\tilde{\boldsymbol{R}}_A = (\tilde{\boldsymbol{r}}_1, \tilde{\boldsymbol{r}}_2, \cdots, \tilde{\boldsymbol{r}}_{13}) = \begin{bmatrix} 1 & 1 & 1 & 0 & 0 & 0 & 0 & 0 & 0 & 0 & 0 & 0 & 0 \\ \tilde{u}-\tilde{c} & \tilde{u} & \tilde{u}+\tilde{c} & 0 & 0 & 0 & 0 & 0 & 0 & 0 & 0 & 0 & 0 \\ \tilde{v} & \tilde{v} & \tilde{v} & 1 & 0 & 0 & 0 & 0 & 0 & 0 & 0 & 0 & 0 \\ \hat{H}-\tilde{u}\tilde{c} & (\tilde{u}^2+\tilde{v}^2)/2 & \tilde{H}+\tilde{u}\tilde{v} & \tilde{v} & \tilde{p} & -1 & -1 & -1 & -1 & 0 & 0 & 0 & 0 \\ \tilde{\varphi}_1 & 0 & \tilde{\varphi}_1 & 0 & 1 & 0 & 0 & 0 & 0 & 0 & 0 & 0 & 0 \\ \tilde{\varphi}_2 & 0 & \tilde{\varphi}_2 & 0 & 0 & 1 & 0 & 0 & 0 & 0 & 0 & 0 & 0 \\ \tilde{\varphi}_3 & 0 & \tilde{\varphi}_3 & 0 & 0 & 0 & 1 & 0 & 0 & 0 & 0 & 0 & 0 \\ \tilde{\varphi}_4 & 0 & \tilde{\varphi}_4 & 0 & 0 & 0 & 0 & 1 & 0 & 0 & 0 & 0 & 0 \\ \tilde{\varphi}_5 & 0 & \tilde{\varphi}_5 & 0 & 0 & 0 & 0 & 0 & 1 & 0 & 0 & 0 & 0 \\ 0 & 0 & 0 & 0 & 0 & 0 & 0 & 0 & 0 & 1 & 0 & 0 & 0 \\ 0 & 0 & 0 & 0 & 0 & 0 & 0 & 0 & 0 & 0 & 1 & 0 & 0 \\ 0 & 0 & 0 & 0 & 0 & 0 & 0 & 0 & 0 & 0 & 0 & 1 & 0 \\ 0 & 0 & 0 & 0 & 0 & 0 & 0 & 0 & 0 & 0 & 0 & 0 & 1 \end{bmatrix}, \tag{24}$$

$$\tilde{\boldsymbol{R}}_B = (\tilde{\boldsymbol{s}}_1, \tilde{\boldsymbol{s}}_2, \cdots, \tilde{\boldsymbol{s}}_{13}) = \begin{bmatrix} 1 & 1 & 1 & 0 & 0 & 0 & 0 & 0 & 0 & 0 & 0 & 0 & 0 \\ \tilde{u} & \tilde{u} & \tilde{u} & 0 & 0 & 0 & 0 & 0 & 0 & 0 & 0 & 0 & 0 \\ \tilde{v}-\tilde{c} & \tilde{v} & \tilde{v}+\hat{c} & 1 & 0 & 0 & 0 & 0 & 0 & 0 & 0 & 0 & 0 \\ \tilde{H}-\tilde{v}\tilde{c} & (\tilde{u}^2+\tilde{v}^2)/2 & \tilde{H}+\tilde{v}\tilde{c} & \tilde{u} & \tilde{p} & -1 & -1 & -1 & -1 & 0 & 0 & 0 & 0 \\ \tilde{\varphi}_1 & 0 & \tilde{\varphi}_1 & 0 & 1 & 0 & 0 & 0 & 0 & 0 & 0 & 0 & 0 \\ \tilde{\varphi}_2 & 0 & \tilde{\varphi}_2 & 0 & 0 & 1 & 0 & 0 & 0 & 0 & 0 & 0 & 0 \\ \tilde{\varphi}_3 & 0 & \tilde{\varphi}_3 & 0 & 0 & 0 & 1 & 0 & 0 & 0 & 0 & 0 & 0 \\ \tilde{\varphi}_4 & 0 & \tilde{\varphi}_4 & 0 & 0 & 0 & 0 & 1 & 0 & 0 & 0 & 0 & 0 \\ \tilde{\varphi}_5 & 0 & \tilde{\varphi}_5 & 0 & 0 & 0 & 0 & 0 & 1 & 0 & 0 & 0 & 0 \\ 0 & 0 & 0 & 0 & 0 & 0 & 0 & 0 & 0 & 1 & 0 & 0 & 0 \\ 0 & 0 & 0 & 0 & 0 & 0 & 0 & 0 & 0 & 0 & 1 & 0 & 0 \\ 0 & 0 & 0 & 0 & 0 & 0 & 0 & 0 & 0 & 0 & 0 & 1 & 0 \\ 0 & 0 & 0 & 0 & 0 & 0 & 0 & 0 & 0 & 0 & 0 & 0 & 1 \end{bmatrix}. \tag{25}$$

For the Grüneisen EOS, $\tilde{\boldsymbol{q}}$, $\tilde{\boldsymbol{A}}$ and $\tilde{\boldsymbol{B}}$ are as follows:

$$\tilde{\boldsymbol{q}} = [\tilde{\rho}, \tilde{\rho}\tilde{u}, \tilde{\rho}\tilde{v}, \tilde{\rho}\tilde{E}, 1/\tilde{\Gamma}, \tilde{p}_{\mathrm{ref}}/\tilde{\Gamma}, \tilde{\rho}\tilde{e}_{\mathrm{ref}}]^{\mathrm{T}}, \tag{26}$$

$$\tilde{\boldsymbol{A}} = \begin{bmatrix} 0 & 1 & 0 & 0 & 0 & 0 & 0 \\ \tilde{K}-\tilde{u}^2 & \tilde{u}(2-\tilde{\Gamma}) & -\tilde{v}\tilde{\Gamma} & \tilde{\Gamma} & -\tilde{p}\tilde{\Gamma} & \tilde{\Gamma} & -\tilde{\Gamma} \\ -\tilde{u}\tilde{v} & \tilde{v} & \tilde{u} & 0 & 0 & 0 & 0 \\ \tilde{u}(\tilde{K}-\tilde{H}) & \tilde{H}-\tilde{u}^2\tilde{\Gamma} & -\tilde{u}\tilde{v}\tilde{\Gamma} & \tilde{u}(\tilde{\Gamma}+1) & -\tilde{u}\tilde{p}\tilde{\Gamma} & \tilde{u}\tilde{\Gamma} & -\tilde{u}\tilde{\Gamma} \\ -\tilde{\varphi}\tilde{u} & \tilde{\varphi} & 0 & 0 & \tilde{u} & 0 & 0 \\ -\tilde{\chi}\tilde{u} & \tilde{\chi} & 0 & 0 & 0 & \tilde{u} & 0 \\ -\tilde{\psi}\tilde{u} & \tilde{\psi} & 0 & 0 & 0 & 0 & \tilde{u} \end{bmatrix},$$

$$\tilde{\boldsymbol{B}} = \begin{bmatrix} 0 & 0 & 1 & 0 & 0 & 0 & 0 \\ -\tilde{u}\tilde{v} & \tilde{v} & \tilde{u} & 0 & 0 & 0 & 0 \\ \tilde{K}-\tilde{v}^2 & \tilde{u}\tilde{\Gamma} & \tilde{v}(2-\tilde{\Gamma}) & \tilde{\Gamma} & -\tilde{p}\tilde{\Gamma} & \tilde{\Gamma} & -\tilde{\Gamma} \\ \tilde{v}(\tilde{K}-\tilde{H}) & -\tilde{u}\tilde{v}\tilde{\Gamma} & \tilde{H}-\tilde{v}^2\tilde{\Gamma} & \tilde{v}(\tilde{\Gamma}+1) & -\tilde{v}\tilde{p}\tilde{\Gamma} & \tilde{v}\tilde{\Gamma} & -\tilde{v}\tilde{\Gamma} \\ -\tilde{\varphi}\tilde{v} & 0 & \tilde{\varphi} & 0 & \tilde{v} & 0 & 0 \\ -\tilde{\chi}\tilde{v} & 0 & \tilde{\chi} & 0 & 0 & \tilde{v} & 0 \\ -\tilde{\psi}\tilde{v} & 0 & \tilde{\psi} & 0 & 0 & 0 & \tilde{v} \end{bmatrix}, \tag{27}$$

where the speed of sound is $\tilde{c} = \sqrt{\tilde{\Gamma}(\tilde{H}-(\tilde{u}^2+\tilde{v}^2)/2-\tilde{p}\tilde{\varphi}+\tilde{\chi}-\tilde{\psi})}$, $\tilde{K} = \tilde{\Gamma}\tilde{u}^2/2$, $\tilde{\varphi} = -\tilde{\Gamma}'/\tilde{\Gamma}^2$, $\tilde{\chi} = (\tilde{\Gamma}\tilde{p}'_{\rm ref} - \tilde{\Gamma}'\tilde{p}_{\rm ref})/\tilde{\Gamma}^2$, $\tilde{\psi} = \tilde{e}_{\rm ref} + \tilde{\rho}\tilde{e}'_{\rm ref}$. The right eigenvector corresponding to eigenvalue of Roe matrix is

$$\tilde{\boldsymbol{R}}_{\boldsymbol{A}} = (\tilde{\boldsymbol{r}}_1, \tilde{\boldsymbol{r}}_2, \ldots, \tilde{\boldsymbol{r}}_7) = \begin{bmatrix} 1 & 1 & 1 & 0 & 0 & 0 & 0 \\ \tilde{u}-\tilde{c} & \tilde{u} & \tilde{u}+\tilde{c} & 0 & 0 & 0 & 0 \\ \tilde{v} & \tilde{v} & \tilde{v} & 1 & 0 & 0 & 0 \\ \tilde{H}-\tilde{u}\tilde{c} & \tilde{K}/\tilde{\Gamma} & \tilde{H}+\tilde{u}\tilde{c} & \tilde{v} & \tilde{p} & -1 & 1 \\ \tilde{\varphi} & 0 & \tilde{\varphi} & 0 & 1 & 0 & 0 \\ \tilde{\chi} & 0 & \tilde{\chi} & 0 & 0 & 1 & 0 \\ \tilde{\psi} & 0 & \tilde{\psi} & 0 & 0 & 0 & 1 \end{bmatrix},$$

$$\tilde{\boldsymbol{R}}_B = (\tilde{\boldsymbol{s}}_1, \tilde{\boldsymbol{s}}_2, \ldots, \tilde{\boldsymbol{s}}_7) = \begin{bmatrix} 1 & 1 & 1 & 0 & 0 & 0 & 0 \\ \tilde{u} & \tilde{u} & \tilde{u} & 1 & 0 & 0 & 0 \\ \tilde{v}-\tilde{c} & \tilde{c} & \tilde{v}+\tilde{c} & 0 & 0 & 0 & 0 \\ \tilde{H}-\tilde{v}\tilde{c} & \tilde{K}/\tilde{\Gamma} & \tilde{H}+\tilde{v}\tilde{c} & \tilde{u} & \tilde{p} & -1 & 1 \\ \tilde{\varphi} & 0 & \tilde{\varphi} & 0 & 1 & 0 & 0 \\ \tilde{\chi} & 0 & \tilde{\chi} & 0 & 0 & 1 & 0 \\ \tilde{\psi} & 0 & \tilde{\psi} & 0 & 0 & 0 & 1 \end{bmatrix}. \tag{28}$$

Having obtained the eigenvector and eigenvalue of the Roe matrix, we can use any high-resolution schemes, similar to dealing with the single-fluid, to calculate the Riemann problem of the multi-fluid flows. In this paper, the second-order Godunov scheme with flux limiter is used in the 1D and 2D examples in the next section.

4. Computational results

4.1. Results of 1D Riemann problem

4.1.1. Riemann problem of two-phase gas-liquid flow with stiffened gas EOS

The first 1D Riemann problem is a problem in shock tube with two-phase gas-liquid flow by stiffened gas EOS (2). We take the same initial data as Refs.[18,19], where on the left side of the interface is the gas $x \in [0, 0.5]$, and on the right side of the interface is the liquid $x \in [0.5, 1.0]$, and we have

$$(\rho \;\; u \;\; p \;\; \gamma \;\; \pi)_{\rm L} = (1.241 \;\; 0 \;\; 2.753 \;\; 1.4 \;\; 0) \qquad x \in [0, 0.5],$$
$$(\rho \;\; u \;\; p \;\; \gamma \;\; \pi)_{\rm R} = (0.991 \;\; 0 \;\; 3.059 \times 10^{-4} \;\; 5.5 \;\; 1.505) \qquad x \in [0.5, 1.0].$$

In Fig.1, the density, pressure and velocity contours in space and time are plotted, and the results for the density, pressure and velocity distributions at time 0.1, where the example has been carried out by using the high-resolution Roe method, with the mesh size of $\Delta x = 1/1000$.

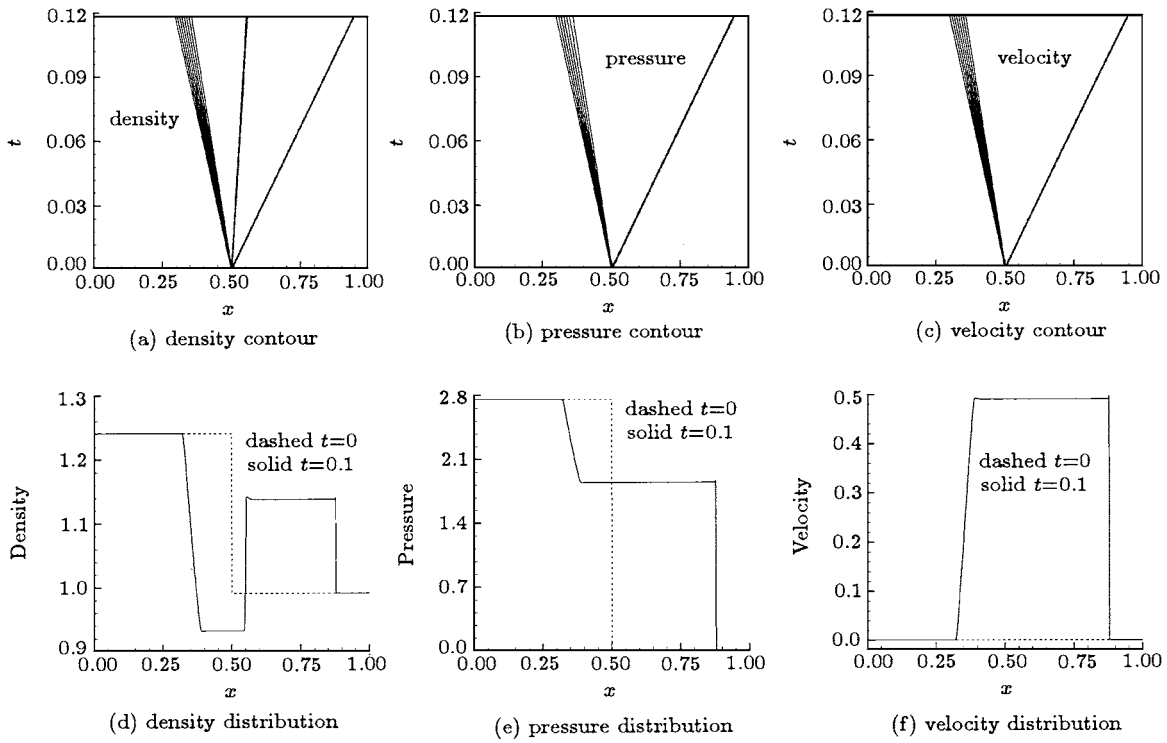


Fig.1. Numerical results for two-phase gas–liquid Riemann problem at t=0.1.

4.1.2. Riemann problem of two gaseous explosives with JWL EOS

The second test problem is a Riemann problem in shock tube with the material inside the tube modelled of two gaseous explosives by the JWL equation of state (7). The material-dependent parameters ρ_0, A, B, R_1, R_2, Γ_0 of the JWL EOS have been listed in Table 1. We take the same initial data as studied by Rider,[20] where on the left side of the interface is PBX-9404, $0 \le x < 1/2\text{m}$, and we have

$$(\rho, u, p, e_0)_{\text{L}} = (1700\text{kg}\cdot\text{m}^{-3}, 0\text{m}\cdot\text{s}^{-1}, 10^{12}\text{Pa}, 0\text{kJ}\cdot\text{kg}^{-1});$$

on the right side of the interface is TATB, $1/2\text{m} \le x \le 1\text{m}$, and we have

$$(\rho, u, p, e_0)_{\text{R}} = (1000\text{kg}\cdot\text{m}^{-3}, 0\text{m}\cdot\text{s}^{-1}, 5\times 10^{10}\text{Pa}, 0\text{kJ}\cdot\text{kg}^{-1}).$$

Table 1. The material-dependent parameters of two gaseous explosives.

JWL EOS	ρ_0/kg·m^{-3}	Γ_0	A/GPa	B/GPa	R_1	R_2
PBX-9404	1842	0.25	852.4	18.02	4.6	1.3
TATB	1900	0.23	654.67	7.12	4.45	1.2

In Fig.2, we show the density, pressure and velocity contours in space and time, as well as the density, pressure and velocity distributions at time 15μs, when the test has been carried out by using the high-resolution Roe method, with the mesh size of $\Delta x = 1/1000$. We obtain excellent resolutions in the region of shock and contact discontinuity. In addition, we can see that our solution is similar to the result in Ref.[20], where a single-component Riemann problem with an approximation Riemann solver based on two-shock approximation was used in computation.

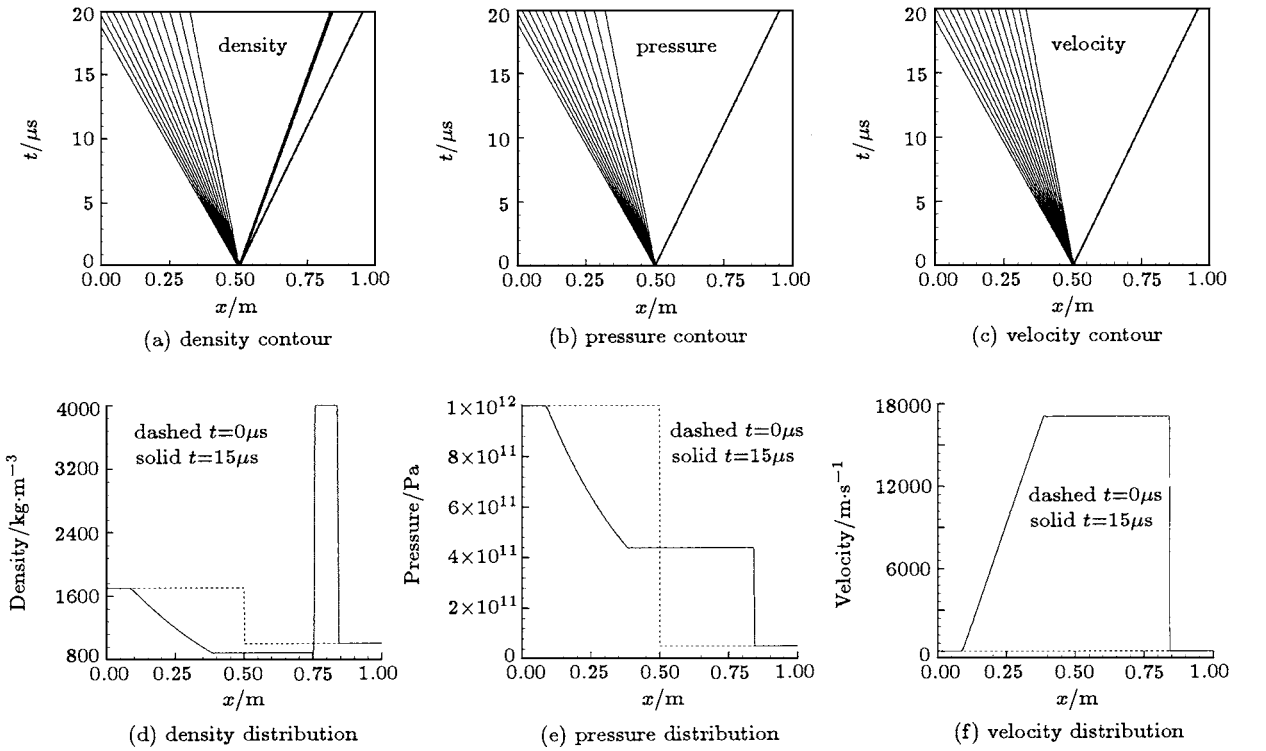


Fig.2. Results for Riemann problem of two gaseous explosives with JWL EOS.

4.1.3. Riemann problem of impact of two metals with Grüneisen and polynomial EOS

The third test problem is a Riemann problem with copper impacting aluminium with a velocity of $2\text{km}\cdot\text{s}^{-1}$. Grüneisen EOS (6) and polynomial EOS (7) are used in calculation for both copper and aluminium. The material-dependent parameters of copper and aluminium with Grüneisen and polynomial EOS are listed in Tables 2 and 3. For comparison, we take the same initial data as follows, where on the left side of the interface, $0 \leq x < 1/2\text{m}$, we have copper:

$$(\rho, u, p)_{\text{L}} = (8924\text{km}\cdot\text{m}^{-1}, 2000\text{m}\cdot\text{s}^{-1}, 0\text{Pa});$$

on the right side of the interface, $1/2\text{m} \leq x \leq 1\text{m}$, we have
aluminium:

$$(\rho, u, p)_{\text{R}} = (2785\text{kg}\cdot\text{m}^{-3}, 0\text{m}\cdot\text{s}^{-1}, 0\text{Pa}).$$

Table 2. The material-dependent parameters of copper and aluminium with Grüneisen EOS[21].

Shock EOS	$\rho_0/\text{kg}\cdot\text{m}^{-3}$	$c_0/\text{m}\cdot\text{s}^{-1}$	λ	Γ_0	α	p_0/Pa	$e_0/\text{kJ}\cdot\text{kg}^{-1}$
Copper	8924.0	3910.0	1.51	2.0	1.0	0.0	0.0
Aluminum	2785.0	5328.0	1.338	1.96	1.0	0.0	0.0

Table 3. The material-dependent parameters of copper and aluminium with polynomial EOS[22].

Polynomial EOS	$\rho_0/\text{kg}\cdot\text{m}^{-3}$	a_1/GPa	a_2/GPa	a_3/GPa	b_0	b_1	b_2	b_3
Copper	8924.0	136.5	138.6	138.9	1.96	0.02	–0.22	0.70
Aluminum	2785.0	79.1	53.1	30.8	2.00	0.005	–0.0688	0.27

It is known that the analytical solution would consist of a rightward going shock wave to the stationary aluminium, and a leftward going shock wave to the moving copper. In Fig.3, we can see that the analytical solution accords excellently with the numerical results for the density, pressure and velocity distributions at time $50\mu\text{s}$ with Grüneisen and polynomial EOS, where the mesh size is Δx=1/1000.

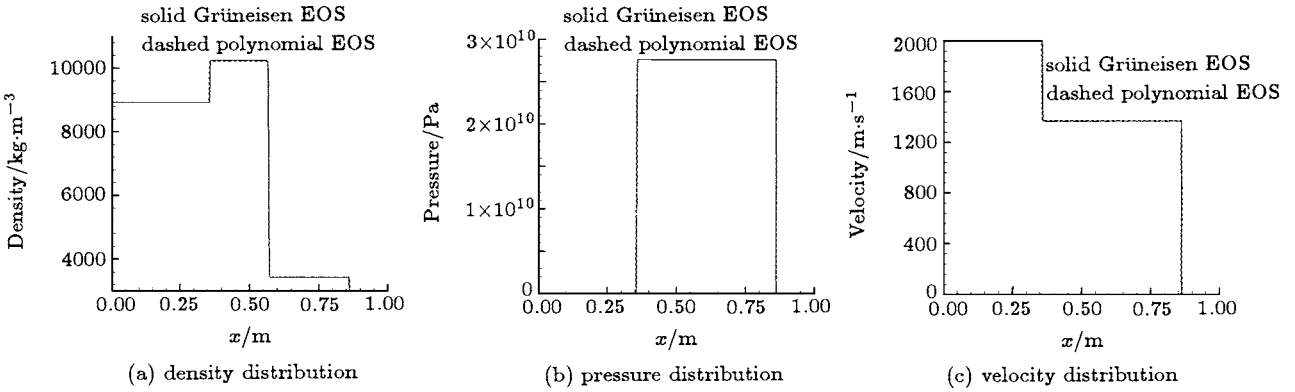


Fig.3. Results for numerical calculation of the impact of two materials with Grüneisen and polynomial EOS.

4.2. Results of 2D Riemann problem

4.2.1. Riemann problem of the stiffened gas

The initial computational domain with $x \in [0,1]$ and $y \in [0,1]$ is divided into four regions by boundaries of $x_0 = 0.8$ and $y_0 = 0.8$, where the I and III are air and the II and IV are helium, see Fig.4. We have (dimensionless)

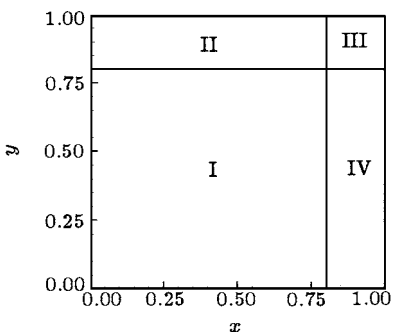


Fig.4. The initial computational domain of the first 2D Riemann problem.

$$(\ \rho \quad u \quad v \quad p \quad \gamma \quad \pi\ ) = \begin{cases} (0.138 \quad 1.206 \quad 1.206 \quad 0.029 \quad 1.4 \quad 0) & \text{in I,} \\ (0.532 \quad 1.206 \quad 0 \quad 0.3 \quad 1.67 \quad 0) & \text{in II,} \\ (1.5 \quad 0 \quad 0 \quad 1.5 \quad 1.4 \quad 0) & \text{in III,} \\ (0.532 \quad 0 \quad 1.206 \quad 0.3 \quad 1.67 \quad 0) & \text{in IV.} \end{cases}$$

For air and helium, the stiffened gas EOS is used. In Fig.5, we show the contours of density, pressure and the resultant velocity at t=0.6, where the plots are symmetrical about the line $x = y$. In addition, a complex wave pattern is formed by the interaction of shock wave and rarefaction wave because of the difference of density and pressure in each of the regions.

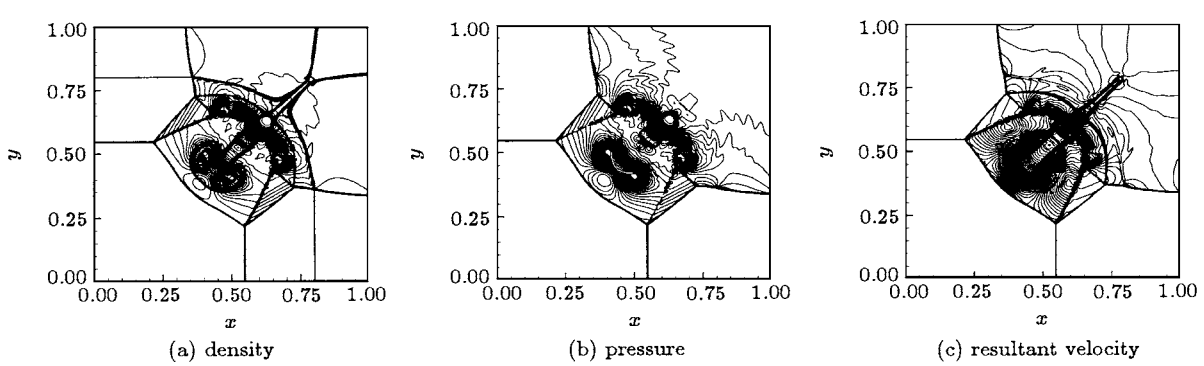


Fig.5. Contours plot for two species Riemann problem at t=0.6.

4.2.2. Riemann problem of two detonation products with JWL EOS

The second 2D Riemann problem is a problem with two detonation products of TATB and PBX-9404 by JWL EOS. The initial computational domain with [0,1m]×[0,1m] is divided into four same regions by the two detonation products where the I and III are full of PBX-9404 product with 7km·s^{-1} and –7km·s^{-1} in x and y directions and the II and IV are TATB product with 8km·s^{-1} and –8km·s^{-1} in x and y directions respectively. We have

$$\begin{aligned}
&\text{I}: \text{PBX}-9404 && (\rho,u,v,p,e_0)_{\text{I}} = (1700\text{kg}\cdot\text{m}^{-3}, 0\text{km}\cdot\text{s}^{-1}, 7.0\text{km}\cdot\text{s}^{-1}, 10^{12}\text{Pa}, 0\text{kJ}\cdot\text{kg}^{-1}),\\
&\text{II}: \text{TATB} && (\rho,u,v,p,e_0)_{\text{II}} = (1300\text{kg}\cdot\text{m}^{-3}, 8.0\text{km}\cdot\text{s}^{-1}, 0\text{km}\cdot\text{s}^{-1}, 8\times10^{11}\text{Pa}, 0\text{kJ}\cdot\text{kg}^{-1}),\\
&\text{III}: \text{PBX}-9404 && (\rho,u,v,p,e_0)_{\text{III}} = (1500\text{kg}\cdot\text{m}^{-3}, \ 0\text{km}\cdot\text{s}^{-1}, -7.0\text{km}\cdot\text{s}^{-1}, 7\times10^{11}\text{Pa}, 0\text{kJ}\cdot\text{kg}^{-1}),\\
&\text{IV}: \text{TATB} && (\rho,u,v,p,e_0)_{\text{IV}} = (1200\text{kg}\cdot\text{m}^{-3}, -8.0\text{km}\cdot\text{s}^{-1}, 0\text{km}\cdot\text{s}^{-1}, 6\times10^{11}\text{Pa}, 0\text{kJ}\cdot\text{kg}^{-1}).
\end{aligned}$$

In Figs.6 and 7, we show the interfacial shape and the contours of density, pressure and resultant velocity at $t = 12\mu$s. Obviously, a vortex clockwise is formed in the centre of the computational domain because of the gradual decrease of the pressure and density from I to IV, as well as influence of the initial velocities distributions.

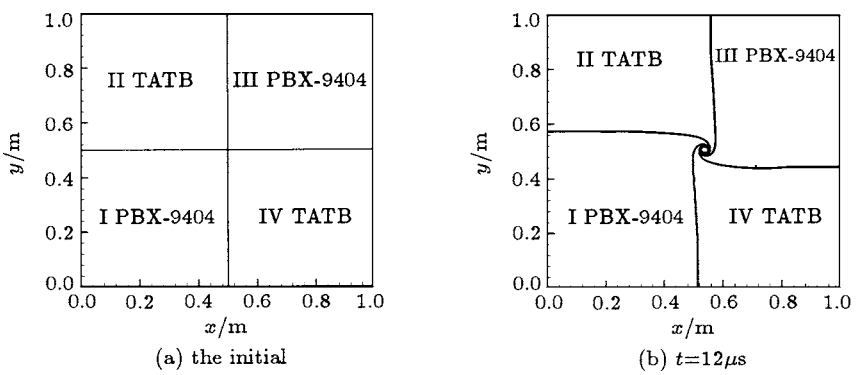


Fig.6. Shapes of the interfaces at the initial state and at t=12μs.

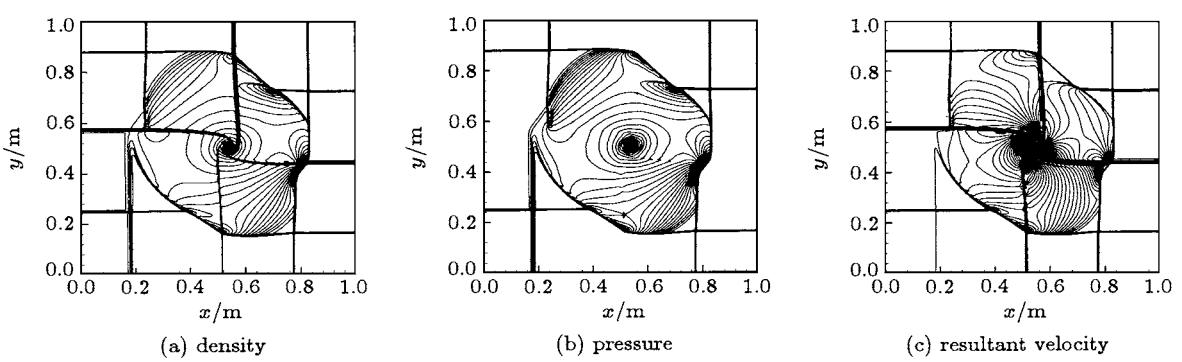


Fig.7. Contours plot for two detonation products Riemann problem at t=12μs.

4.2.3. Riemann problem of three-materials interaction with Grüneisen EOS

The third 2D Riemann problem is a problem with copper, solid explosive and water by Grüneisen EOS. The initial computational domain is [0m, 1m]×[0m, 1m], where the copper is arranged in [0.6m, 1m]×[0m, 1m], the solid explosive is arranged in [0m, 0.6m]×[0.5m, 1m] and the rest is the water (Fig.8). Initially, copper impact the stationary explosive and

water with $-1.5\text{km}\cdot\text{s}^{-1}$ velocity in x direction. We take the parameters of EOS in Table 2, and the parameters of EOS for the solid explosive and water are extracted from Refs.[21,22] (Table 4). Figure 9 shows the contours of the density, pressure and the resultant velocity at t=50μs, 100μs.

In this case, the shock wave propagates in the three materials at different speeds. Since the acoustic impedance of the solid explosive is greater than that of water, we can find that the shock wave propagates faster in solid explosive than in water. At the same time, because of the head-on collision between the leading edge of the copper plate and the water-explosive interface, generation of a reflected circular wave is observed.

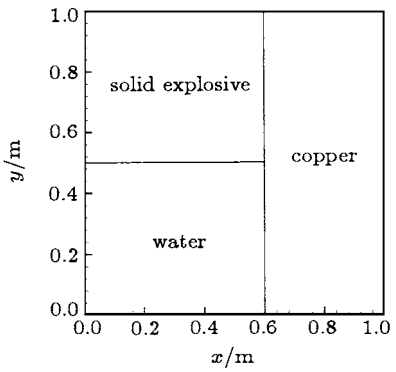


Fig.8. Computational model.

Table 4. The material-dependent parameters of solid explosive and water with Grüneisen EOS[21,22].

shock EOS	$\rho_0/\text{kg}\cdot\text{m}^{-3}$	$c_0/\text{m}\cdot\text{s}^{-1}$	λ	Γ_0	α	p_0/Pa	$e_0/\text{kJ}\cdot\text{kg}^{-1}$
water	1000.0	1483.0	2.0	2.0	0.0001	0.0	0.0
solid JWL	$\rho_0/\text{kg}\cdot\text{m}^{-3}$	Γ_0	A/GPa	B/GPa	R_1	R_2	–
TNT	1840.0	0.93	12.87	13.42	4.1	3.1	–

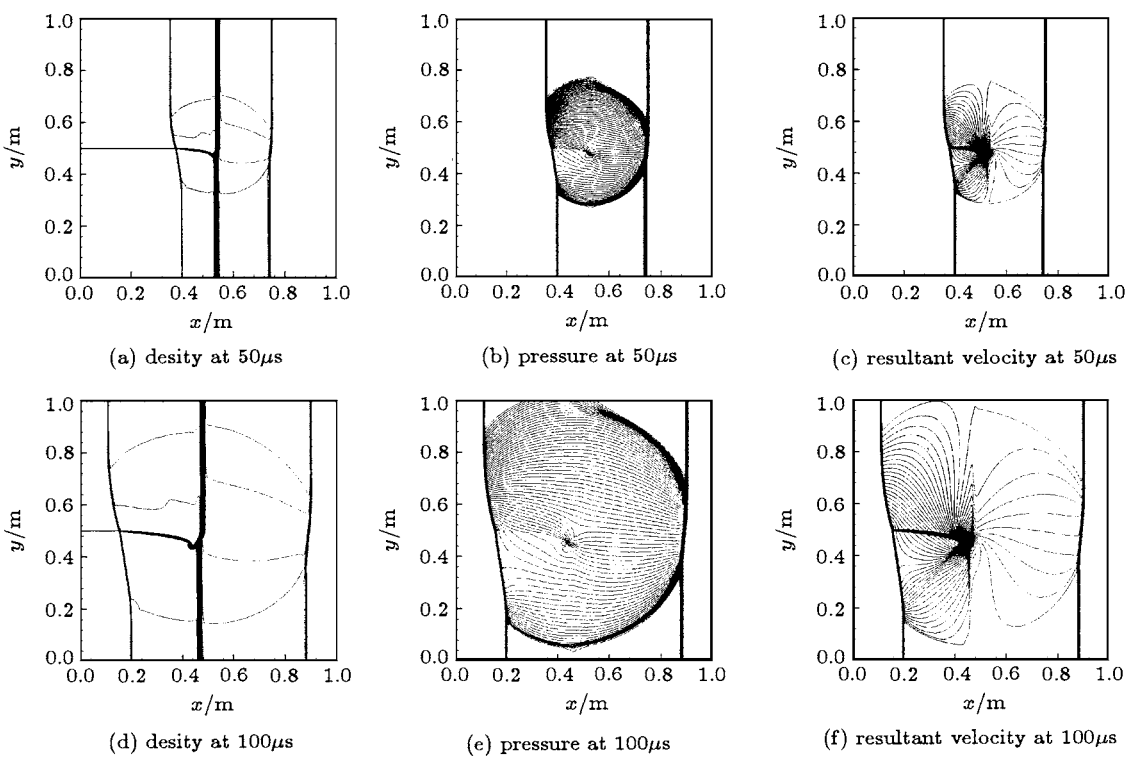


Fig.9. Density, pressure and resultant velocity contours plot at t=50μs, 100μs.

5. Conclusion

In order to solve the Riemann problem for multi-fluid compressible flows with general EOS, we adopt the high-resolution numerical scheme which is used successfully in single-fluid flows, deduce a set of interface capture equations according to the general equation of state, couple the hydrodynamic conservation equations with interface capture equations to-

gether and construct the Roe matrix and eigenvector of quasi-linear equations. This method in our paper is successful for the Riemann problem of multi-fluid flow with ideal gas, stiffened gas, polynomial and Grüneisen EOS, and is verified through a series of numerical results.

References

[1] Miller G H and Puckett E G 1996 *J. Comput. Phys.* **128** 134

[2] Menikoff R and Plohr B J 1989 *Rev. Mod. Phys.* **61** 75

[3] Balsara D S 1994 *J. Comput. Phys.* **114** 284

[4] Glaister P 1988 *J. Comput. Phys.* **74** 382

[5] Quirk J J 1994 *Int. Numer. Methods. Fluids* **18** 555

[6] Schulz-Rinne C W, Collins J P and Glaz H M 1993 *SIAM J. Sci. Comput.* **14** 1394

[7] Karni S 1996 *SIAM J. Sci. Comput.* **17** 1019

[8] Guo W B, Wang N C, Shi B C and Guo Z L 2003 *Chin. Phys.* **12** 67

[9] Bai J S, Li P, Zhang Z J, Hua J S and Tan H 2004 *Chin. Phys.* **13** 1992

[10] Xu Y S, Wu F M, Chen Y Y and Xu X Z 2003 *Chin. Phys.* **12** 621

[11] Noh W F and Woodward P 1976 *Lecture Notes in Physics* (Berlin: Springer)

[12] Puckett E G and Saltzman J S 1992 *Phys.* D **60** 84

[13] Hirt C W and Nichels B D 1981 *J. Comput. Phys.* **39** 201

[14] Youngs D L *Time Dependent Multi-material Flow with Large Fluid Distortion* In: Morton K W and Baines M J eds 1982 *Numerical Methods for Fluid Dynamics* p277

[15] Yan Z Y and Zhang H Q 2001 *J. Phys.* A 34 1785

[16] Li B, Chen Y, Xuan H N and Zhang H Q 2004 *Appl. Math. Comput.* **152** 581

[17] Hong W P and Park S H 2004 *Int. J. Mod. Phys.* C **15** 363

[18] Cocchi J P, Saurel R and Loraud J C 1996 *Shock Waves* **5** 347

[19] Cooke C H and Chen T J 1991 *J. Sci. Comput.* **6** 269

[20] Rider W J 1999 *Comput. Fluids* **28** 741

[21] Marsh S P 1980 *LASL Shock Hugoniot Data* (Berkeley: University of California Press)

[22] Wilkins M L 1999 *Computer Simulation of Dynamic Phenomena* (New York: Springer)